

# $\Lambda$ -hypernuclear production in $(K_{\text{stop}}^-, \pi)$ reactions\*

VOJTĚCH KREJČÍŘÍK

Nuclear Physics Institute, Řež, Czech Republic  
Faculty of Mathematics and Physics, Charles University, Prague, Czech Republic

AND

ALEŠ CIEPLÝ

Nuclear Physics Institute, Řež, Czech Republic

We report on calculation of the  $\Lambda$  - hypernuclear production induced by the stopped  $K^-$ . The calculation was performed within the framework of the distorted wave impulse approximation and employed chirally motivated model for the microscopic description of the elementary  $K^-$ -nucleon process. The sensitivity of the calculation was tested with various wave functions of both the kaon in the initial state and the pion in the final state. Our results are closer to the experimental values than the results of previous calculations.

PACS numbers: 13.75.Jz, 21.80.+a, 25.80.Nv

## 1. Introduction

We studied the  $\Lambda$ -hypernuclear production induced by the stopped kaon,  $(K_{\text{stopped}}^-, \pi)$ . We believe that an analysis of this process can provide additional information on a depth of the  $K^-$ -nucleus potential, whether it is deep or shallow. Previous calculations [1, 2, 3] did not give satisfactory predictions, the capture rates were at least three times smaller than the experimental values. The novelty in our approach is mainly a microscopic description of the elementary process using a chirally motivated model. Moreover, we studied the sensitivity of the calculation to various input wave functions.

---

\* This work was supported by the GAUK grant No. 91509 and the GACR grant No. 202/09/1441

## 2. Formalism

We used a distorted wave impulse approximation (DWIA) as described in detail by Gal and Klieb [1]. The T-matrix is written in a form

$$T_{\text{if}}(\mathbf{q}_f) = t_{\text{if}}(\mathbf{q}_f) \int d^3\mathbf{r} \chi_{q_f}^*(\mathbf{r}) \rho_{\text{if}}(\mathbf{r}) \Psi_{NLM}(\mathbf{r}) . \quad (1)$$

Here,  $t_{\text{if}}(\mathbf{q}_f)$  denotes the t-matrix of the elementary process,  $\Psi_{NLM}(\mathbf{r})$  and  $\chi_{q_f}(\mathbf{r})$  are the  $K^-$  and  $\pi$  wave functions,  $\mathbf{q}_f$  is the pion momentum, and  $\rho_{\text{if}}$  stands for the nucleus to hypernucleus transition density matrix.

The capture rate per one stopped kaon  $R_{\text{if}}$  is defined as a ratio of the capture rate for a specific process to the total capture rate. After some manipulations (see [1]), the final formula for  $R_{\text{if}}$  can be expressed as a product of three terms:

$$R_{\text{if}} = \frac{q_f \omega_f}{\bar{q}_f \bar{\omega}_f} \cdot R(K^- N \rightarrow \pi Y) \cdot R_{\text{if}}/Y. \quad (2)$$

The first term is a kinematical factor, the second represents the branching ratio for the elementary process and the third, which we call the capture rate per hyperon, reads

$$R_{\text{if}}/Y = \frac{\int \frac{d\Omega_{q_f}}{4\pi} \left\langle \left| \int d^3r \chi_{q_f}^{(-)*}(\mathbf{r}) \rho_{\text{if}}(\mathbf{r}) \Psi_{NLM}(\mathbf{r}) \right|^2 \right\rangle}{\tilde{\rho}_N}, \quad (3)$$

where

$$\tilde{\rho}_N = \int d^3\mathbf{r} \rho_N(r) \rho_{K^-}(r) \rho_\pi(r) \quad (4)$$

is called the effective nucleon density. Following Gal and Klieb [1] one should replace the pion distribution by a simple plane wave ( $\rho_\pi = 1$ ) in Eq. (4) in order to account for all possible final states contributing to the total capture rate. We also looked at the effect of keeping the pion distortion in Eq. (4). It leads to a substantial increase of the calculated capture rates and to a better agreement with experimental data. Although we find this feature interesting, such modification is not consistent with the DWIA approach and therefore cannot be taken seriously.

The factor  $R_{\text{if}}/Y$  is evaluated analytically using the spherical coordinates and the partial wave expansion. The final form reads

$$R_{n_N l_N \rightarrow n_Y l_Y}/Y = \frac{N(j_N) \sum_k (2k+1) (l_N 0 k 0 | l_Y 0) N_{\gamma_Y \gamma_N}^{(k)}}{\int dr \rho_N(r) |R_{NL}(r)|^2}, \quad (5)$$

where

$$N_{\gamma_Y \gamma_N}^{(k)} = \sum_l (L 0 k 0 | l 0)^2 |I_{\gamma_Y \gamma_N}^l|^2 ,$$

$N(j_N)$  is the number of nucleons in the shell  $j_N$ , and  $I_{\gamma_Y \gamma_N}^l$  stands for the overlap of the radial parts of the wave functions of  $K^-$ ,  $N$ ,  $\pi$ , and  $Y$ .

### 3. Inputs

In this chapter, we present the elementary branching ratios and potentials used to determine the wave functions of  $K^-$ ,  $\pi$ ,  $N$  and  $Y$ .

#### 3.1. Elementary branching ratios

In order to describe the elementary  $K^-$ -nucleon process, we adopted the effective potential model based on chiral symmetry. The details of the approach can be found in Refs. [4, 5, 6, 7]. In the calculation, we took account of the Pauli blocking [5] and the  $K^-$ -selfenergy [3]. The pertinent elementary branching ratios evaluated at the  $K^-N$  threshold are  $R(K^-n \rightarrow \pi^- \Lambda) = 10.72$ , and  $R(K^-p \rightarrow \pi^0 \Lambda) = 5.36$ .

#### 3.2. Wave functions

To calculate the  $K^-$ -atomic wave function, we used an optical potential, which describes the strong interaction, in addition to the electromagnetic interaction (including finite size charge distribution and vacuum polarization effects). The strong interaction  $K^-$ -nucleus potential is taken in the form devised in Ref. [8],

$$V_{opt}^K(r) = -\frac{4\pi}{2\mu} \left(1 + \frac{\mu}{M_N}\right) \left[ b + B \left( \frac{\rho(r)}{\rho(0)} \right)^\nu \right] \rho(r). \quad (6)$$

We used three different parameter sets, which are specified in Table 1. The choice  $[K_\chi]$  represents the chiral model [6],  $[K_{\text{eff}}]$  and  $[K_{\text{DD}}]$  denote phenomenological potentials taken from Ref. [8]. For a reference, we also show the respective potential depths in the last column of the table. Moreover, we also performed the calculation with a pure electromagnetic potential ( $[K_{\text{EM}}]$ ) to check the impact of the strong interaction.

Table 1. Parameters of the kaonic optical potential.

set	$b$ [fm]	$B$ [fm]	$\nu$	$V_{opt}^K(\rho = \rho_0)$ [MeV]
$[K_\chi]$	$0.38 + 0.48i$	0	0	50
$[K_{\text{eff}}]$	$0.63 + 0.89i$	0	0	80
$[K_{\text{DD}}]$	$-0.15 + 0.62i$	$1.65 - 0.06i$	0.23	190

The baryon wave functions were obtained using Wood-Saxon potential with parameters fixed to reproduce single particle binding energies. The

pion-nucleus optical potential is taken in the standard form [9]. We performed our calculations for a free pion ( $\pi_0$ ) and for two different parameter sets, ( $\pi_b$ ) [10] and ( $\pi_c$ ) [11], which describe the low energy pion scattering data.

#### 4. Results and discussion

In this chapter, we present our results and discuss the sensitivity of the calculated capture rates to the choice of the  $K^-$ -nucleus and  $\pi$ -nucleus potential. We focus on the production of  $\Lambda$  - hypernuclei ( ${}^{12}_{\Lambda}\text{C}$ ,  ${}^{12}_{\Lambda}\text{B}$ ,  ${}^{16}_{\Lambda}\text{O}$ ,  ${}^{16}_{\Lambda}\text{N}$ ) and take into account the hyperon formation in both the  $1S$  and the  $1P$  states.

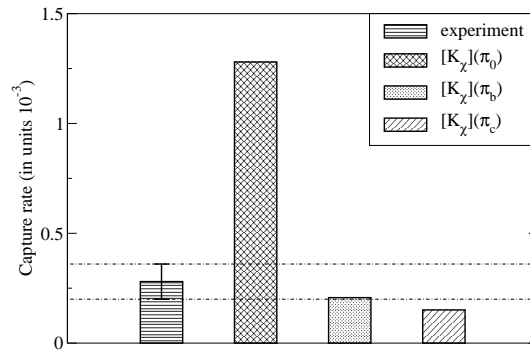


Fig. 1. The production of  ${}^{12}_{\Lambda}\text{B}$  in the  $1S_{\Lambda}$  state.

First, we look at the effect of various pion wave functions. Our results are shown in Fig.1. One can see that the inclusion of the pion distortion, no matter whether ( $\pi_b$ ) or ( $\pi_c$ ), leads to a substantial decrease of the capture rate  $R_{\text{if}}$  (up to one order). Apparently, the final state interaction plays an important role. On the other hand, it looks that the computed rates are not very sensitive to the choice of pion-nucleus optical potential.

The sensitivity of the capture rates to the choice of  $K^-$  wave functions is demonstrated in Fig.2. It appears that the capture rate is a decreasing function of the  $K^-$  - nucleus potential depth.

To determine the best combination of potentials involved in our work, we compare our results with the available experimental data for the production of  ${}^{12}_{\Lambda}\text{C}$  [12],  ${}^{12}_{\Lambda}\text{B}$  [13], and  ${}^{16}_{\Lambda}\text{O}$  [14]. In the comparison, we include six production rates to the  $1S_{\Lambda}$  and  $1P_{\Lambda}$  states and four ratios between them. The resulting  $\chi^2$  per data point are shown in Table 2. The best value is achieved for the combination of the  $[K_{\chi}]$  and ( $\pi_b$ ) potentials. It is interesting that comparable (if not even better) results are obtained with the kaon

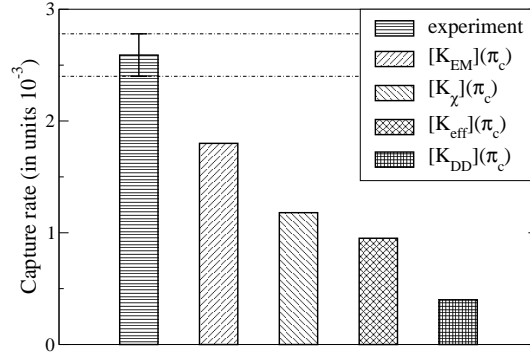


Fig. 2. The production of  $^{12}_\Lambda\text{C}$  in the  $1P_\Lambda$  state.

wave function generated by a purely electromagnetic interaction (the choice  $[K_{EM}]$ ).

Table 2. The comparison of various combinations of potentials.

$\chi^2/N$	$[K_{EM}]$	$[K_\chi]$	$[K_{eff}]$	$[K_{DD}]$
$(\pi_0)$	206.7	219.9	166.0	79.3
$(\pi_b)$	7.3	<b>7.7</b>	11.7	20.0
$(\pi_c)$	7.9	10.0	14.2	31.3

The comparison of our results with experimental data [12, 13, 14] and with the previous calculations is given in Fig.3. The predictions made by Gal and Klieb [1] are labeled GL, by Matsuyama and Yazaki [2] MY, and by Cieply et al. [3] CFGM. Apparently, our results are closer to the experimental data than the results of previous works.

## 5. Conclusion

We performed the calculation of the  $\Lambda$  - hypernuclear production making use of a microscopic model for the description of the elementary process. We showed that the capture rate is a decreasing function of the kaon-nucleus potential depth and that our model based on the DWIA is very sensitive to pion distortion in the final state.

Our results are closer to the experimental data than the results of previous calculations. It looks that the shallow potential  $[K_\chi]$  is the best in the description of the hypernuclear production. Unfortunately, the ambiguities in the input wave functions and in other factors involved in the theory make this statement very weak and do not allow us to decide convincingly which potential (deep  $[K_{DD}]$  or shallow  $[K_\chi]$ ) is better in general.

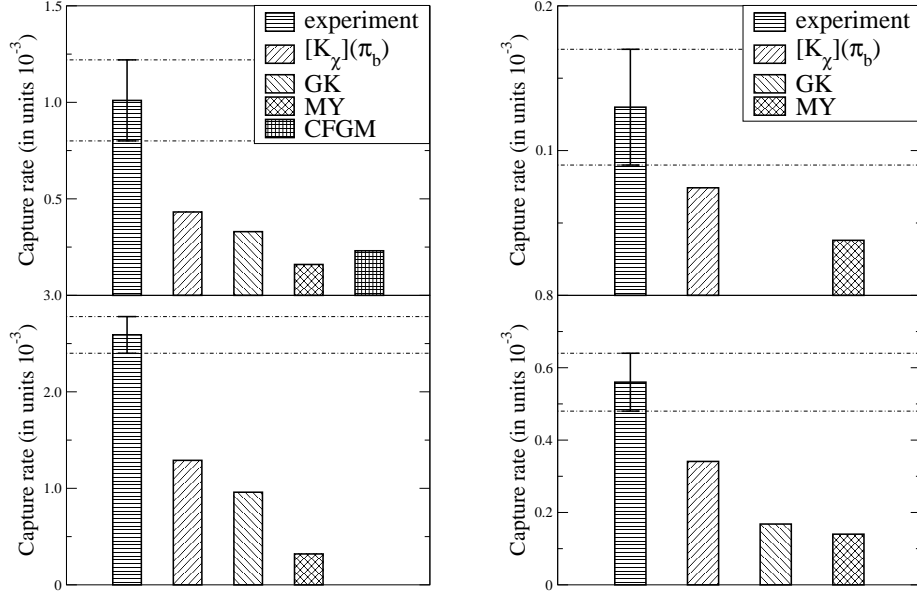


Fig. 3. The production of  $^{12}\text{C}$  (left) and  $^{16}\text{O}$  (right) in the  $1S_\Lambda$  (top) state and in the  $1P_\Lambda$  state (bottom).

## REFERENCES

- [1] Gal A., Klieb L.: Phys. Rev. C **34**, 956 (1986).
- [2] Matsuyama A., Yazaki K.: Nucl. Phys. A **477**, 6 (1988).
- [3] Cieplý A., Friedman E., Gal A., Mareš J.: Nucl. Phys. A **696**, 173 (2001).
- [4] Kaiser N., Siegel P.B., Weise W.: Nucl. Phys. A **594**, 325 (1995).
- [5] Waas T., Kaiser N., Weise W.: Phys. Lett. B **365**, 12 (1996).
- [6] Cieplý A., Smejkal J.: Eur. Phys. J. A **34**, 237 (2007).
- [7] Cieplý A., Smejkal J.: arXiv:0910.1822 (2009).
- [8] Friedmann E., Gal A., Batty C.J.: Nucl. Phys. A **696**, 173 (1994).
- [9] Ericson M., Ericson T.E.O.: Ann. of Phys. **36**, 323 (1966).
- [10] Thiessen H. A. et al.: LAMPF Report no. LA-7607-PR (1978).
- [11] Harvey C. J. et al.: LAMPF Report no. LA-UR-84-1732 (1984).
- [12] M. Agnello et al., Phys. Lett. B **622**, 35 (2005).
- [13] Ahmed M.W., Cui X., Empl. A., et al.: Phys. Rev. C **68**, 64004-1 (2003).
- [14] Tamura H., Hayano R.S., Outa H., Yamazaki T.: Prog. Theor. Phys. Suppl. **117**, 1 (1994).